Initial Value Diffeomorphic Landmark Matching and Its Application to Shape Statistics

Marc Vaillant, Michael Miller, Laurent Younes, and Alain Trouvé*

We study the well established diffeomorphic landmark matching problem central to the emerging field of computational anatomy [1, 2, 3], emphasizing a point of view which enables a new optimization approach and setting for stochastic shape models. The diffeomorphic landmark matching problem is formulated as follows. Let Ω be an open, bounded subset of $\mathbb{R}^k$ and consider an N-tuple, $x = (x_1, \ldots, x_N)$ of template landmarks in Ω and a corresponding N-tuple of target landmarks $y = (y_1, \ldots, y_N)$. We seek to find an optimal diffeomorphism, $\phi : \Omega \to \Omega$, which maps the template landmark configuration onto the target. As candidates, we consider only the family of diffeomorphisms, G, that are isotopic to the identity via solutions to the ODE

$$\frac{\partial \phi}{\partial t} = v_t \circ \phi_t,$$

where for each $t \in [0, 1]$, v_t belongs to a reproducing kernel Hilbert space, V, of vector fields on Ω with

$$\int_0^1 ||v_t||_V dt < \infty.$$

Let $x_i(t)$ denote $\phi_t(x_i)$. The optimal diffeomorphism is chosen by finding the time varying velocity field $v \in L^1([0, 1], V)$ minimizing the following energy functional

$$\int_0^1 ||v_t||_V^2 dt + \frac{1}{\sigma^2} \sum_{i=1}^N ||x_i(1) - y_i||^2_{\mathbb{R}^k}. \qquad (1)$$

The Euler equations characterizing the extremals of the energy can be shown to be equivalent to the system (2) above top right, where K is the matrix reproducing kernel of V having the property $\langle K(x)u, v \rangle_V = v(x) \cdot u$. Our main contribution is to take advantage of the fact that, from system (2), the flow is completely determined by the initial conditions $x_i(0)$ and $a_i(0)$ (or $v_0(x_i)$). In fact, (2) has a conservation of momentum physical interpretation, with the initial conditions $a_i(0)$ representing the initial momentum [4]. We compute the gradient of the energy functional (1) with respect to the initial conditions $a_i(0)$ and implement gradient descent minimization. The top row in the right figure illustrates a large deformation example with $N = 2$, in which the landmarks trajectories must cross. The template is in blue and the target is in red. The top left panel shows the initial conditions resulting from the gradient descent minimization. The top right panel shows the landmark trajectories computed via (2), and below it is a sampled sequence from the deformation flow of a grid. Also shown to the right are 2D (above) and 3D (below) face examples (2D data from AAM database [5], and 3D data from the Morphable Faces database [6]). The left panels show the template configurations, with the flow sequence in the center panels and the targets in the right panels.

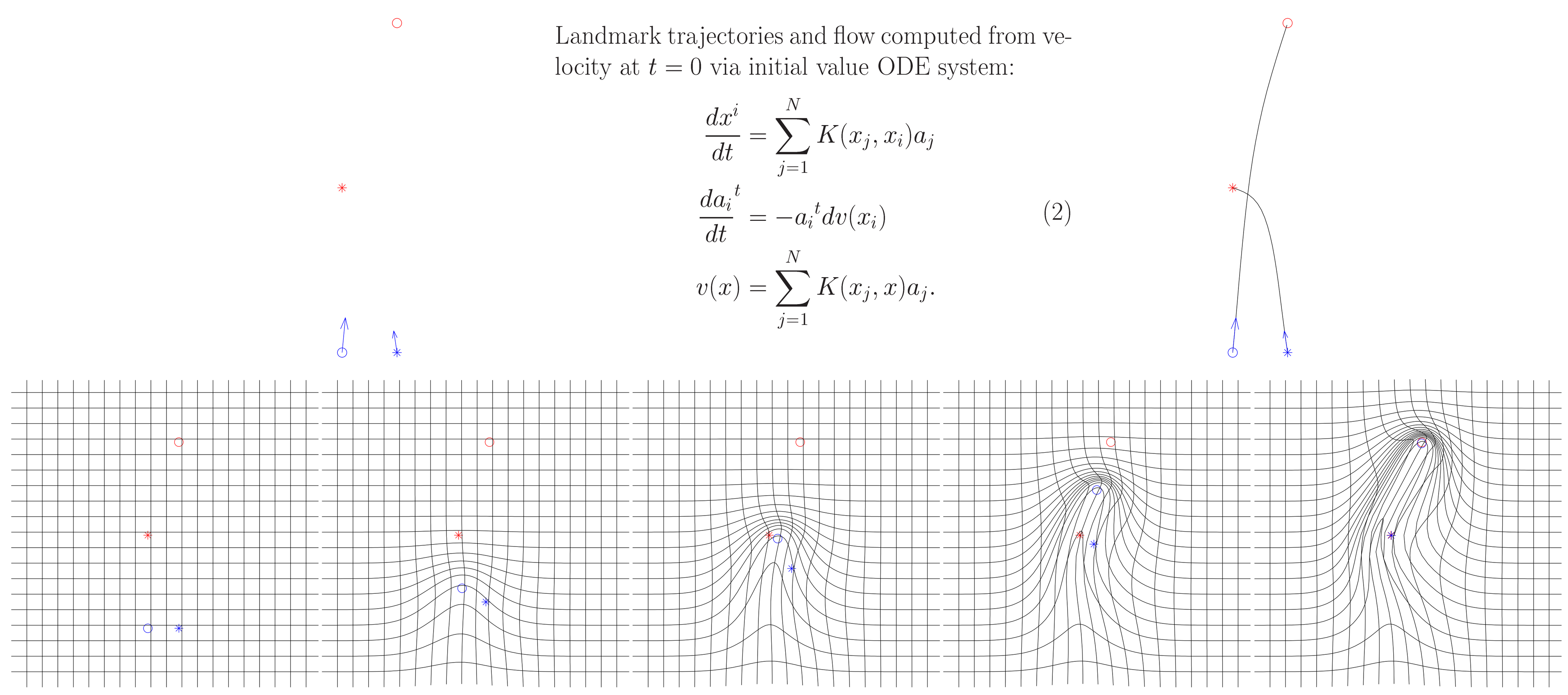

Landmark trajectories and flow computed from velocity at $t = 0$ via initial value ODE system:

$$\frac{dx^i}{dt} = \sum_{j=1}^N K(x_j, x_i) a_j$$
$$\frac{d{a_i}^t}{dt} = -{a_i}^t dv(x_i) \qquad (2)$$
$$v(x) = \sum_{j=1}^N K(x_j, x) a_j.$$

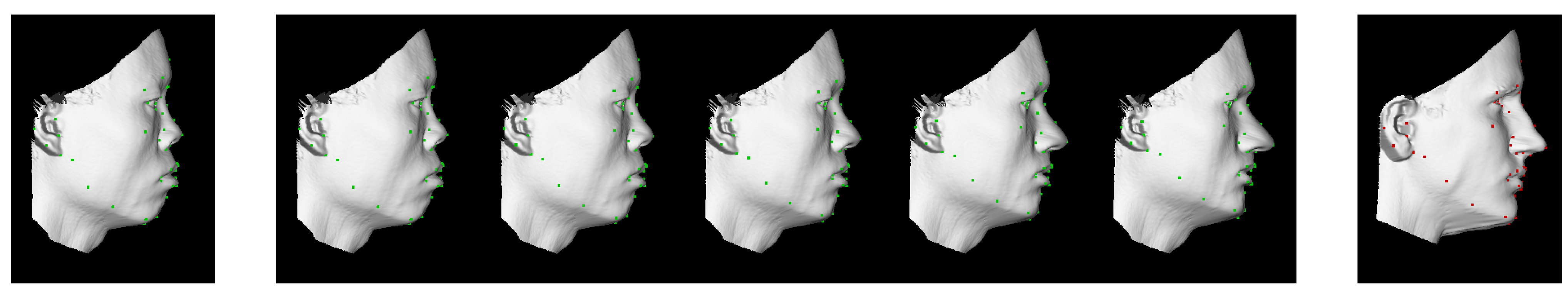

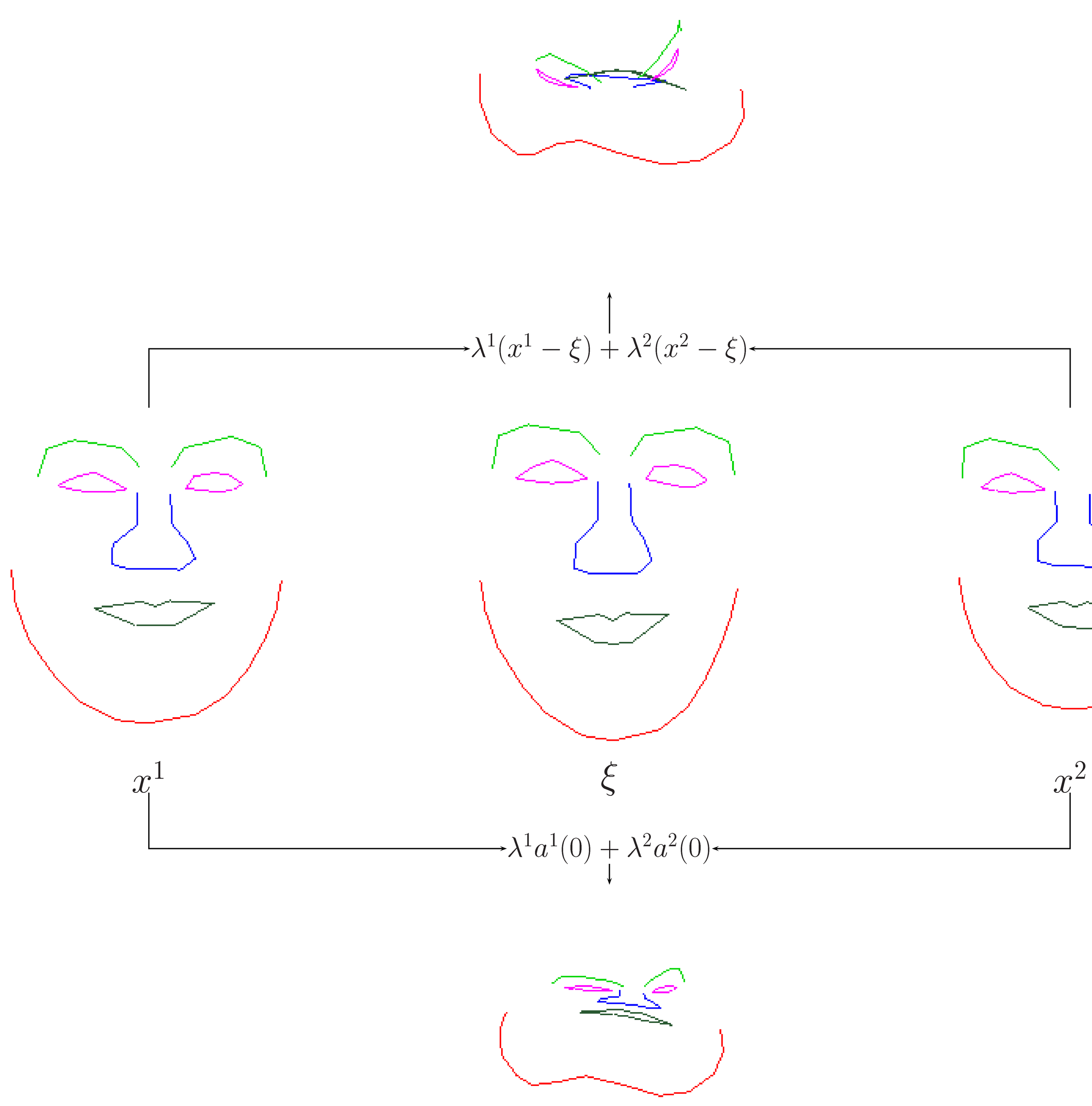

An additional consequence of the initial value system is that it provides dimensionality reduction for shape statistics [7] and active shape models [8] in the large deformation setting. The solutions to (1) are actually geodesics in G (an infinite dimensional Riemannian manifold), which induce a metric on the space of landmark configurations. The metric distance in terms of initial momentum is given by

$$d(x, y) = \Big(\sum_{i=1}^N a_i(0) \cdot v_0(x_i) \Big)^{\frac{1}{2}}.$$

As well, the space of initial momentum allows us to overcome the non-linearity problem evident in active shape models. The figure on the left shows three landmark models from the AAM 2D data set [5]. We arbitrarily choose the center model, ξ, as a hypothetical mean and left, x^1, and right, x^2, models as hypothetical eigen modes. The top figure is a resulting linear combination of x^1 and x^2 about ξ. Clearly, this linear combination produces a configuration which does not represent a face. The mouth appears above the nose and the structures run into one another, etc. The bottom figure is produced by taking the corresponding linear combination of the resulting initial conditions, $a^1(0)$ and $a^2(0)$ which take ξ to x^1 and x^2, and applying (2) to compute the flow from the new initial condition. The topological structure of the face is clearly retained.

We have experimented with mean shape estimation using a procrustean type algorithm. Consider a set of landmark configurations $\{y^1, \ldots, y^M\}$:

1. Choose a template ξ arbitrarily.
2. Compute the diffeomorphisms from ξ to y^m for $m = 1, \ldots, M$.
3. Set $a(0) = \frac{1}{M} \sum_{m=1}^M a^m(0)$.
4. Compute $\phi_1(\xi)$ via (2) using $a(0)$ as the initial condition.
5. Set $\xi = \phi_1(\xi)$ and goto step 2.

Empirically, this algorithm appears to converge with mean estimates independent of the initial choice of template.

References

[1] U. Grenander and M. I. Miller. Computational anatomy: An emerging discipline. *Quarterly of Applied Mathematics*, pages 617–694, 1998.

[2] S. C. Joshi and M. I. Miller. Landmark matching via large deformation diffeomorphisms. *IEEE Transactions on Image Processing*, 9(8):1357–1370, August 2000.

[3] M.I. Miller, A. Trouvé, and L. Younes. On the metrics and Euler-Lagrange equations of computational anatomy. *Annual Review of Biomedical Engineering*, 4:375–405, 2002.

[4] M.I. Miller, A. Trouvé, and L. Younes. Geodesic shooting for computational anatomy. *In review.*

[5] M. B. Stegmann. Analysis and segmentation of face images using point annotations and linear subspace techniques. Technical report, Informatics and Mathematical Modelling, Technical University of Denmark, DTU, August 2002.

[6] V. Blanz and T.A. Vetter. Morphable model for the synthesis of 3D faces. *SIGGRAPH '99 Conference Proceedings*, pages 187–194, 1999.

[7] F.L. Bookstein. *Morphometric Tools for Landmark Data.* Cambridge University Press, New York, 1991.

[8] A. Hill, T.F. Cootes, and C.J. Taylor. Active shape models and the shape approximation problem. *Image and Vision Computing*, 14(8):601–608, August 1996.

* CMLA, École Normale Supérieure de Cachan, 61 Avenue du President Wilson, F-94235, Cachan, CEDEX, France

Center for Imaging Science **http://www.cis.jhu.edu**

Research supported by NSF DMS-0219016,
NIH 1 P41 RR15241-01A1, NIH 1 P41 RR15241-01A1